LETTERS

Small regulatory RNAs inhibit RNA polymerase II during the elongation phase of transcription

Shouhong Guang[1], Aaron F. Bochner[1], Kirk B. Burkhart[1], Nick Burton[1], Derek M. Pavelec[2] & Scott Kennedy[1,2]

Eukaryotic cells express a wide variety of endogenous small regulatory RNAs that regulate heterochromatin formation, developmental timing, defence against parasitic nucleic acids and genome rearrangement. Many small regulatory RNAs are thought to function in nuclei[1,2]. For instance, in plants and fungi, short interfering RNA (siRNAs) associate with nascent transcripts and direct chromatin and/or DNA modifications[1,2]. To understand further the biological roles of small regulatory RNAs, we conducted a genetic screen to identify factors required for RNA interference (RNAi) in *Caenorhabditis elegans* nuclei[3]. Here we show that the gene nuclear RNAi defective-2 (*nrde-2*) encodes an evolutionarily conserved protein that is required for siRNA-mediated silencing in nuclei. NRDE-2 associates with the Argonaute protein NRDE-3 within nuclei and is recruited by NRDE-3/siRNA complexes to nascent transcripts that have been targeted by RNAi. We find that nuclear-localized siRNAs direct an NRDE-2-dependent silencing of pre-messenger RNAs (pre-mRNAs) 3′ to sites of RNAi, an NRDE-2-dependent accumulation of RNA polymerase (RNAP) II at genomic loci targeted by RNAi, and NRDE-2-dependent decreases in RNAP II occupancy and RNAP II transcriptional activity 3′ to sites of RNAi. These results define NRDE-2 as a component of the nuclear RNAi machinery and demonstrate that metazoan siRNAs can silence nuclear-localized RNAs co-transcriptionally. In addition, these results establish a novel mode of RNAP II regulation: siRNA-directed recruitment of NRDE factors that inhibit RNAP II during the elongation phase of transcription.

We previously described a forward genetic screen for factors required for RNAi in *C. elegans* nuclei[3]. This screen identified the Argonaute (Ago) protein NRDE-3, which transports siRNAs from the cytoplasm to the nucleus[3]. Here we report that this screen identified 28 mutant alleles defining the gene *nrde-2*, which was required for RNAi processes within nuclei. For instance, wild-type *C. elegans*

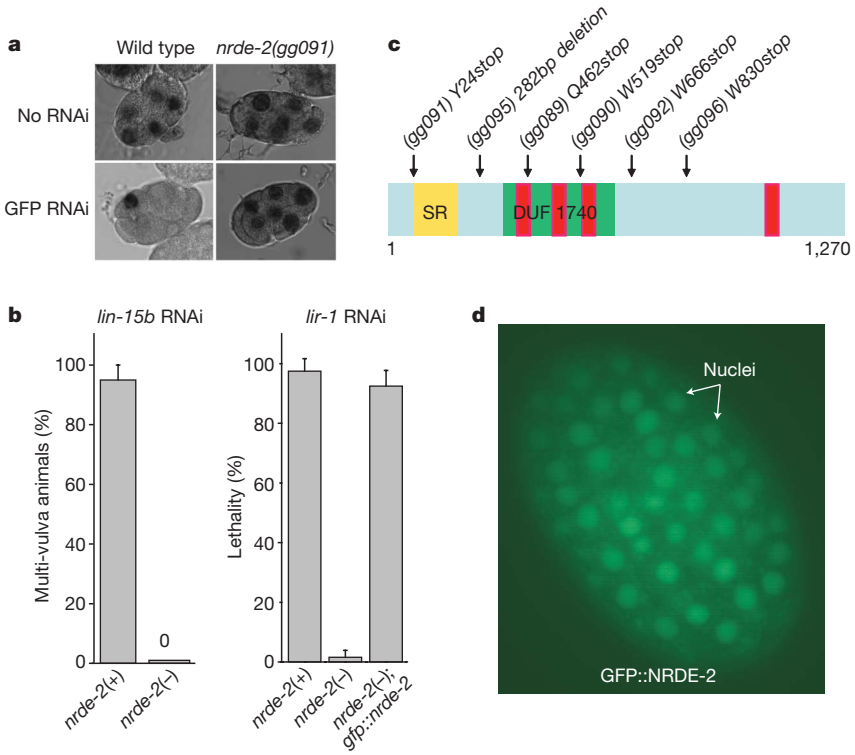

Figure 1 | The gene *nrde-2* encodes a conserved and nuclear-localized protein that is required for nuclear RNAi. a, Light microscopy of embryos of about six cells with or without GFP RNAi subjected to *in situ* hybridization detecting *pes-10::gfp* RNA. **b**, *nrde-2*(−) animals fail to silence the *lin-15b/lin15a* and *lir-1/lin-26* nuclear-localized RNAs ($n = 4$; bars, s.d.). An *eri-1*(−) genetic background was used for this analysis. **c**, Predicted domain structure of NRDE-2. Yellow, serine/arginine domain; green, DUF1740; red, potential HAT-like repeats. **d**, Fluorescent microscopy of an embryo of about 200 cells expressing a rescuing GFP::NRDE-2 fusion protein.

[1]Laboratory of Genetics, University of Wisconsin, Madison, Wisconsin 53706, USA. [2]Department of Pharmacology, University of Wisconsin, Madison, Wisconsin 53706, USA.

animals silence the nuclear-retained *pes-10::GFP* mRNA after exposure to double-stranded RNA (dsRNA) targeting this *pes-10::GFP* mRNA (green fluorescent protein (GFP) RNAi)[3,4]. *nrde-2* mutant animals failed to silence the *pes-10::GFP* mRNA after GFP RNAi, indicating that a wild-type copy of *nrde-2* is required for dsRNA-mediated silencing of this nuclear-localized RNA (Fig. 1a and Supplementary Fig. 2). The *lin-15b* and *lin-15a* genes are expressed as a bicistronic RNA, which is separated into distinct *lin-15b* and *lin-15a* RNAs within the nucleus. Animals lacking both *lin-15b* and *lin-15a*, but not either gene product alone, exhibit a multi-vulva (Muv) phenotype[5,6]. RNAi targeting *lin-15b* alone is sufficient to induce a Muv phenotype, indicating that nuclear-localized *lin-15b/a* RNA can be silenced by RNAi[3]. *nrde-2*(−) animals failed to exhibit a Muv phenotype in response to *lin-15b* RNAi (Fig. 1b). Similarly, *nrde-2* was required for silencing the nuclear-localized *lir-1/lin-26* polycistronic RNA (Fig. 1b and Methods). Thus *nrde-2* is required for RNAi-based silencing of these nuclear-localized RNAs.

To determine the molecular identity of *nrde-2*, we mapped *nrde-2* to a genetic interval containing the gene T01E8.5. Sequencing of T01E8.5 from six independent *nrde-2* mutant strains identified six mutations in T01E8.5 (Fig. 1c). Transformation of wild-type T01E8.5 DNA into *nrde-2* mutant animals rescued *nrde-2* mutant phenotypes (Fig. 1b). Thus, T01E8.5 corresponds to *nrde-2*, which encodes an approximately 130-kDa protein (NRDE-2) containing a conserved domain of unknown function (DUF) 1740, and two domains frequently found in RNA processing factors: a serine/arginine-rich domain and half-a-tetratricopeptide (HAT)-like domains (Fig. 1c and Supplementary Fig. 3). A single putative orthologue of NRDE-2 was found in plant, fission yeast, insect and mammalian genomes[7]. A fusion gene between GFP and NRDE-2 (*gfp::nrde-2*), which was sufficient to rescue *nrde-2*(−) mutant phenotypes (Fig. 1b), localized predominantly to the nucleus (Fig. 1d). Finally, animals harbouring putative null alleles of *nrde-2* produce approximately 25% of the number of progeny that wild-type animals do (Supplementary Fig. 4). We conclude that *nrde-2* encodes a conserved and nuclear-localized protein that is important for fecundity and is required for nuclear RNAi.

We sought to clarify the relationship between NRDE-2 and the Ago protein NRDE-3. Genetic analyses demonstrated that *nrde-2* and *nrde-3* function in the same genetic pathway (Fig. 2a). NRDE-2, however, was not required for NRDE-3 to transport siRNAs from the cytoplasm to the nucleus; NRDE-3 bound siRNAs and, in response to siRNA binding, localized to the nucleus similarly in both *nrde-2*(+) and *nrde-2*(−) animals (Fig. 2b). These data suggest that NRDE-2 may function downstream of NRDE-3-mediated siRNA transport during nuclear RNAi. In support of this hypothesis, we observed a weak, but reproducible, association between NRDE-3 and NRDE-2; NRDE-3 co-precipitated 0.1–0.5% of the total cellular pool of NRDE-2 (Fig. 2c). Conversely, NRDE-3 co-precipitated with NRDE-2 (Supplementary Fig. 5). An NRDE-3 variant harbouring mutations within its nuclear localization signal (termed NRDE-3(*NLS)) localizes constitutively to the cytoplasm[3]. NRDE-2 did not co-precipitate with NRDE-3(*NLS) (Fig. 2c). Taken together, these data show that NRDE-2 functions downstream of NRDE-3/siRNA transport in the nuclear RNAi pathway and associates with NRDE-3 in the nucleus.

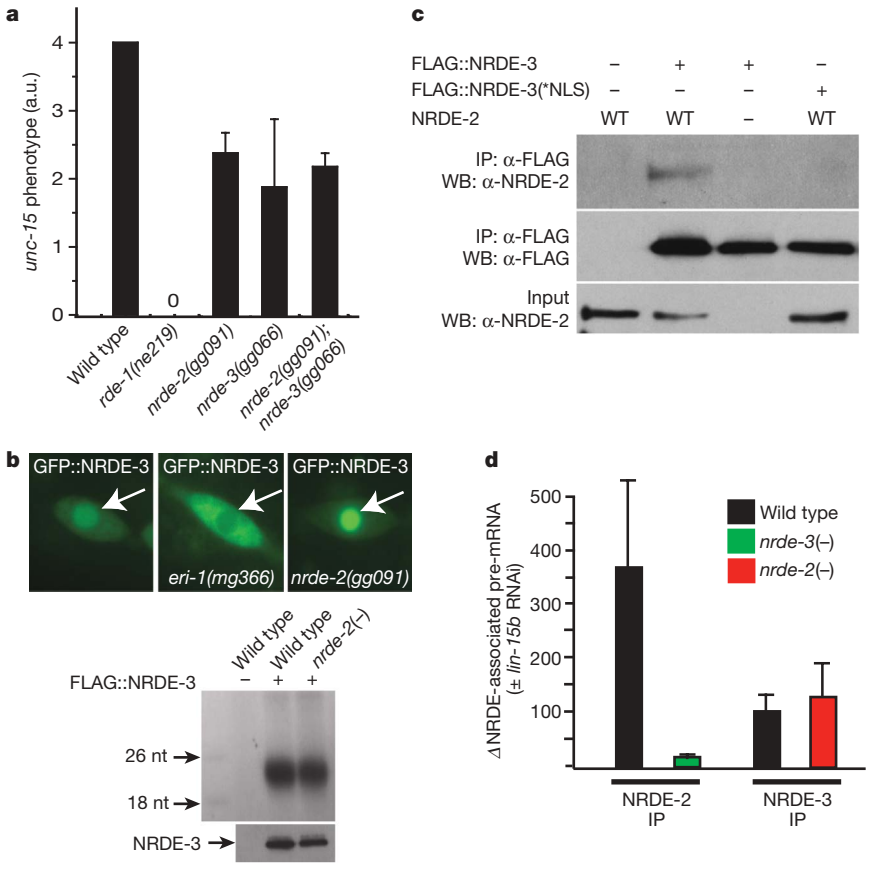

Figure 2 | NRDE-2 is recruited by NRDE-3/siRNA complexes to pre-mRNAs that have been targeted by RNAi. **a**, Animals were exposed to *unc-15* dsRNA and scored for uncoordinated phenotypes (Unc) ($n = 3$; bars, s.d.). *rde-1(ne219)* animals are defective for RNAi[12]. **b**, Top panels: fluorescent microscopy of a seam cell expressing GFP::NRDE-3. Arrows indicate nuclei. *eri-1(mg366)* animals fail to express endo-siRNAs and consequently NRDE-3 is mislocalized to the cytoplasm[3,13,14]. Bottom panels: FLAG::NRDE-3 co-precipitating RNAs radiolabelled with ^{32}P and analysed by polyacrylamide gel electrophoresis. **c**, NRDE-2 co-precipitates with nuclear-localized NRDE-3 (Methods) ($n = 3$). **d**, rtPCR quantification of NRDE-2/3 co-precipitating pre-mRNA. Throughout this paper, pre-mRNA levels are quantified with exon–intron or intron–intron primer pairs. Data are expressed as ratios of co-precipitating pre-mRNA with or without *lin-15b* RNAi ($n = 4$ for NRDE-2 IP, $n = 2$ for NRDE-3 IP; bars, s.e.m.). Δ, fold change.

siRNAs direct NRDE-3 to bind pre-mRNAs that have been targeted by RNAi. For instance, after RNAi targeting *lir-1*, *unc-40* or *dpy-28*, we detected a greater than 200-fold increase in the amount of *lir-1*, *unc-40* or *dpy-28* pre-mRNA that co-precipitated with NRDE-3, respectively (Supplementary Fig. 6)[3]. The RNAi-directed association of NRDE-3 with pre-mRNA depends upon the ability of NRDE-3 to bind siRNAs and the ability of NRDE-3 to localize to the nucleus[3]. NRDE-2 was not required for NRDE-3 to associate with pre-mRNA: in *nrde-2*(+) and *nrde-2*(−) animals NRDE-3 was recruited to pre-mRNAs with similar efficiency (Fig. 2d). As *nrde-2*(−) animals are disabled for nuclear RNAi, these data indicate that the recruitment of NRDE-3/siRNA complexes to pre-mRNAs is not sufficient to trigger nuclear silencing. Interestingly, RNAi also directed NRDE-2 to pre-mRNAs; *lin-15b* RNAi induced a greater than 300-fold increase in the amount of *lin-15b* pre-mRNA that co-precipitated with NRDE-2 (Fig. 2d). The RNAi-mediated recruitment of NRDE-2 to pre-mRNA was dependent upon NRDE-3; more than 10-fold less pre-mRNA co-precipitated with NRDE-2 in *nrde-3*(−) animals than in *nrde-3*(+) animals (Fig. 2d). Similar results were obtained when an endogenous pre-mRNA target of the NRDE pathway was analysed (Supplementary Fig. 7). Taken together, these data indicate that, after RNAi, NRDE-2 is recruited to pre-mRNAs by NRDE-3, which itself is localized to pre-mRNAs by siRNA/pre-mRNA base pairing.

To further our understanding of nuclear RNAi, we conducted a reverse genetic screen for nuclear RNAi factors (Supplementary Fig. 8). This screen identified *nrde-2* and *nrde-3*, as well as five additional putative nuclear RNAi factors (Supplementary Fig. 8). Rpb7 is a subunit of RNAP II that functions in siRNA-mediated heterochromatin formation in *Schizosaccharomyces pombe*[8]. Our screen identified the *C. elegans* orthologue of Rpb7 (*rpb-7*); RNAi of *rpb-7* induced nuclear RNAi defects similar to those induced by RNAi of *nrde-2* or *nrde-3* (Fig. 3a and Supplementary Fig. 8). The identification and characterization of mutant alleles of *C. elegans rpb-7* will be required to confirm a role for *rpb-7* in *C. elegans* nuclear RNAi. Nonetheless, these data hint that nuclear RNAi may act concurrently with RNAP II transcription in *C. elegans*.

Five additional lines of investigation cumulatively indicate that nuclear RNAi operates during the elongation phase of transcription. First, pre-mRNA splicing is thought to occur co-transcriptionally[9]. Therefore, the association of NRDE-2/3 with unspliced RNAs suggests that nuclear RNAi operates near or at the site of transcription (Fig. 2d). Second, we subjected animals undergoing RNAi to chromatin immunoprecipitation (ChIP) detecting tri-methylated (me3) H3K9 and found that RNAi directed an NRDE-2-dependent enrichment of H3K9me3 at a genomic site targeted by RNAi (Fig. 3b and Supplementary Fig. 9). These data establish that, as in other organisms, *C. elegans* siRNAs direct H3K9 methylation, and support the idea that nuclear RNAi in *C. elegans* operates in close proximity to the site of transcription. Third, we isolated RNA from animals subjected to RNAi targeting *lin-15b*, *lir-1* or *dpy-28* and measured pre-mRNA abundance at multiple sites distributed across the length of these pre-mRNAs, respectively. RNAi resulted in NRDE-2-dependent silencing of these pre-mRNAs 3′ to the site of RNAi (Fig. 3c and Supplementary Fig. 10). These data show that nuclear RNAi is unlikely to occur at the initiation phase of transcription. Rather, they imply that nuclear RNAi operates during transcription elongation. Incidentally, these data also show that, for unknown reasons, the relative contribution of the nuclear RNAi pathway to overall RNAi-based silencing can vary, depending on the gene targeted by RNAi (Supplementary Fig. 10)[3]. Fourth, after bouts of *dpy-28* RNAi, NRDE-2 and NRDE-3 associated with *dpy-28* pre-mRNA fragments encoded upstream (5′) of the site of RNAi with more than 200-fold greater efficacy than sequences encoded downstream (3′) of the site of RNAi (Fig. 3d). Similar results were obtained after *lin-15b*, *lir-1* and *unc-40* RNAi (Supplementary Fig. 11). Nuclear silencing events were required for the preferential association of NRDE-3 with 5′ pre-mRNA fragments; in *nrde-2*(−) animals, NRDE-3 associated with pre-mRNA sequences encoded both 5′ and 3′ to the site of RNAi with equal efficiency (Supplementary Fig. 11c). These data support the

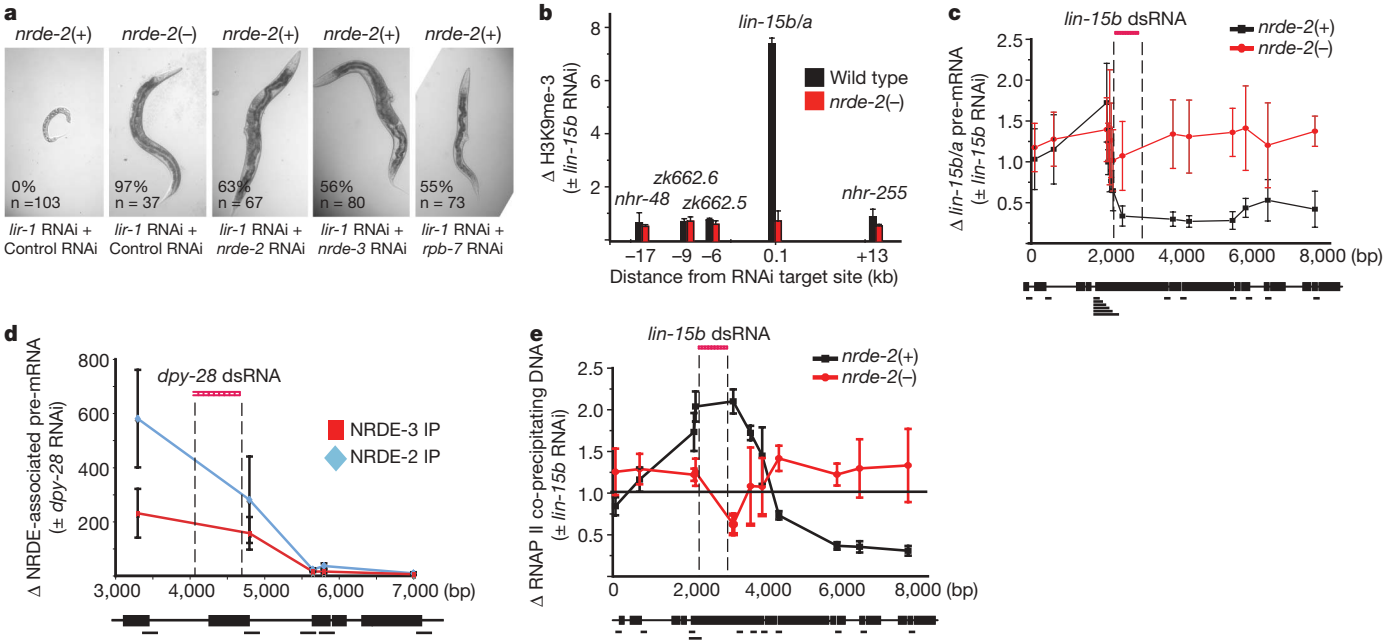

Figure 3 | *C. elegans* siRNAs direct an NRDE-2/3-dependent co-transcriptional gene silencing program. a, Animals were exposed to one part *lir-1* dsRNA expressing bacteria and six parts vector control, *nrde-2/3* or *rpb-7* dsRNA expressing bacteria. The percentage of animals that failed to exhibit *lir-1* RNAi phenotypes is indicated. **b**, ChIP with H3K9me3 antibody (Upstate, 07-523). Data are expressed as the ratio of H3K9me3 co-precipitating DNA with or without *lin-15b* RNAi ($n = 2$; bars = s.d.). **c**, Total RNA was isolated and *lin-15b* pre-mRNA was quantified with rtPCR. Data are expressed as ratios with or without *lin-15b* RNAi. The genetic background was *eri-1*(−) (bars = s.d.). **d**, FLAG::NRDE-2/3 co-precipitating *dpy-28* pre-mRNA. Data are expressed as ratios with or without *dpy-28* RNAi ($n = 4$; bars, s.d.). **e**, ChIP of AMA-1/Rpb1 with α-AMA-1 antibody (Covance, 8WG16). Data are expressed as ratios of AMA-1 co-precipitating DNA with or without *lin-15b* RNAi ($n = 3$; bars, s.d.). The genetic background was *eri-1*(−).

idea that nuclear RNAi silences pre-mRNAs during the elongation phase of transcription, and suggest that NRDE-2/3 remain associated with pre-mRNA fragments after silencing. Fifth, we subjected animals undergoing RNAi to ChIP targeting the largest subunit of RNAP II, AMA-1/Rpb1. AMA-1/Rpb1 occupancy increased near genomic regions targeted by RNAi (Fig. 3e and Supplementary Fig. 12). No changes in RNAP II occupancy were observed near sites of transcription initiation. Increases in AMA-1/Rpb1 occupancy were dependent upon NRDE-2; *nrde-2*(−) animals did not exhibit changes in AMA-1/Rpb1 occupancy after RNAi (Fig. 3e and Supplementary Fig. 12). Thus RNAi elicits NRDE-2-dependent increases in AMA-1/Rpb1 occupancy at or near genomic sites targeted by RNAi, indicating that siRNAs regulate RNAP II elongation. Taken together, these data indicate that *C. elegans* siRNAs, acting in conjunction with NRDE-2/3, silence nascent transcripts during the elongation phase of transcription.

Interestingly, we detected a decrease in AMA-1/Rpb1 occupancy downstream of the site of *lin-15b* (and to a lesser extent *lir-1*) RNAi, suggesting that siRNAs might inhibit RNAP II transcription (Fig. 3e and Supplementary Fig. 12). Two additional lines of evidence support this hypothesis. First, we quantified *lin-15b* pre-mRNA associated with RNAP II before and after *lin-15b* RNAi. *lin-15b* RNAi decreased the amount of *lin-15b* pre-mRNA that co-precipitated with RNAP II. This effect was dependent upon NRDE-2, and was observed 3′, but not 5′, to the site of RNAi (Fig. 4a). Second, we established a *C. elegans* nuclear run-on assay using 5-bromouridine 5′-triphosphate (Br-UTP). This approach detected *lin-15b* transcription, which was sensitive to the RNAP II inhibitor α-amanitin (Fig. 4b); *ama-1(m118m526)* encodes a mutant variant of AMA-1/Rbp1 that is resistant to α-amanitin[10]. Transcription from *ama-1(m118m526)* nuclei was insensitive to α-amanitin treatment (Fig. 4b). Finally, *lin-15b* transcription was not detected when reactions were performed with nuclei harbouring a *lin-15b* deletion allele (Fig. 4b). Thus our nuclear run-on assay measures RNAP II-mediated transcription of the *lin-15b* locus. *lin-15b* RNAi induced an NRDE-2/3-dependent inhibition of RNAP II transcription 3′ to the site of *lin-15b* RNAi (Fig. 4c and Supplementary Fig. 13). siRNA-directed RNAP II inhibition was observed approximately 2 kilobases downstream of the site of RNAi, hinting that (after recruitment of NRDE-2) additional molecular events may be required to silence RNAP II. Shifting the location of RNAi towards the 5′ end of the *lin-15b* gene resulted in a coincident shift in patterns of RNAP II inhibition, indicating that the response of RNAP II to RNAi was sequence-directed and sequence-specific (Supplementary Fig. 14). Finally, *lir-1* RNAi directed a similar NRDE-2-dependent inhibition of RNAP II transcription downstream of the site of *lir-1* RNAi (Fig. 4d). We conclude that siRNAs direct an NRDE-2/3-dependent inhibition of RNAP II activity that occurs during the elongation phase of transcription. It should be noted that the decreases in RNAP II occupancy and RNAP II activity that we observe 3′ to sites of RNAi indicate that siRNAs, acting in conjunction with NRDE-2/3, are likely to terminate RNAP II transcription.

Transcription is a highly regulated process. Here we describe a novel mechanism by which transcription can be regulated: small regulatory RNA-dependent recruitment of NRDE factors that inhibit RNAP II during the elongation phase of transcription. Eukaryotic cells express a multitude of small regulatory RNAs and antisense transcripts that are of unknown function. It will be interesting to test whether these RNAs regulate RNAP II by the mechanism described here. The mechanism of nuclear silencing in *C. elegans* is enigmatic. Many Ago proteins function by endonucleolytic cleavage of target RNAs (slicer activity)[11]. The Ago protein NRDE-3 lacks residues required for slicer activity, indicating that nuclear RNAi in *C. elegans* is unlikely to depend upon NRDE-3-mediated slicing of pre-mRNAs[3,12]. We have shown that nuclear RNAi silences pre-mRNAs co-transcriptionally and that nuclear RNAi inhibits RNAP II elongation and transcription. Thus our data suggest a mechanism for nuclear RNAi: siRNA-directed co-transcriptional silencing of RNAP II. Alternatively, the RNAP II inhibition that we observe may represent a secondary consequence of another (currently unknown) co-transcriptional silencing activity associated with the NRDE pathway.

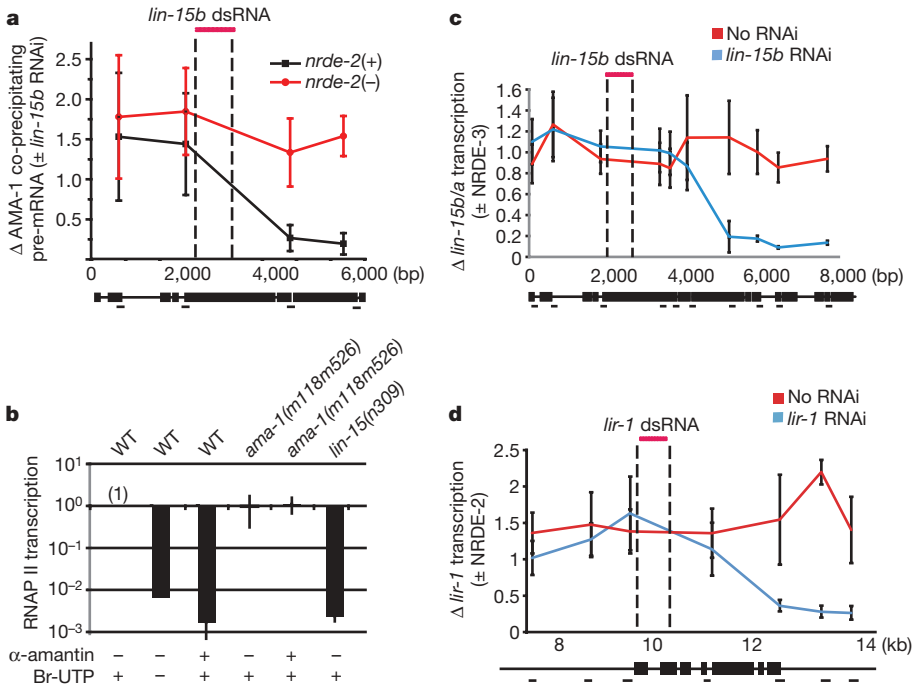

Figure 4 | siRNAs direct an NRDE-2/3-dependent inhibition of RNAP II during the elongation phase of transcription. **a**, AMA-1 co-precipitating pre-mRNA. Data are expressed as ratio with or without *lin-15b* RNAi ($n = 3$; bars, s.d.). **b**, A crude preparation of nuclei was subjected to nuclear run-on analysis (see Methods). Transcription detected from wild-type (WT) nuclei was defined as one ($n = 3$; bars, s.d.). **c**, **d**, RNAi inhibits RNAP II activity 3′ to sites of RNAi. An *eri-1*(−) genetic background was used for these analyses. Nuclei isolated from animals treated with *lin-15b* (**c**) or *lir-1* (**d**) RNAi were subjected to run-on analysis. Data are expressed as ratio of transcription detected in *nrde-3*(+)/*nrde-3*(−) nuclei (**c**) or *nrde-2*(+)/*nrde-2*(−) nuclei (**d**) ($n = 5$ for **c**, $n = 3$ for **d**; bars, s.e.m.).

Finally, NRDE-2 is directed to nascent transcripts by siRNAs and NRDE-2 is required for linking siRNAs to RNAP II inhibition. NRDE-2 is conserved. It will therefore be interesting to assess whether small regulatory RNAs and RNAP II are similarly linked in other metazoans.

METHODS SUMMARY

The following strains were used for this work: (YY151) *eri-1(mg366); nrde-2(gg091)*, (YY158) *nrde-3(gg066)*, (YY174) *ggIS1*[*nrde-3p::3xflag::gfp::nrde-3*], (YY178) *eri-1(mg366); ggIS1*, (YY186) *nrde-2(gg091)*, (YY197) *nrde-2(gg091)*; *axIs36*[*pes-10::gfp*], (YY229) *nrde-2(gg091); ggIS1*, (YY258) *nrde-2(gg091); nrde-3(gg066)*, (YY298) *nrde-3(gg066); ggIS24*[*nrde-3p::3xflag::gfp::nrde-3*nls*], (YY323) *eri-1(mg366); nrde-2(gg091); unc-119(ed3); ggIS28*[nrde-3p::3xflag::gfp::nrde-2], (YY346), *nrde-2(gg091); ggIS28*, (YY353) *nrde-2(gg091); ggIS1*; *ggIS36*[*nrde-3p::3xha::gfp::nrde-2*], (YY363) *nrde-3(gg066); nrde-2(gg091); ggIS28*, (GR1373) *eri-1(mg366)*, (WM27) *rde-1(ne219)*, (DR1099) *ama-1(m118m526)*, (MT309) *lin-15AB(n309)*, (JH103) *axIs36*. Worm culture conditions, plasmid construction, feeding RNAi assay, *lir-1* RNAi assay, RNA *in situ* hybridization, fluorescence imaging, complementary DNA (cDNA) preparation, NRDE-2/3 co-precipitation, RNA immunoprecipitation, RNA isolation, quantitative real-time PCR (rtPCR), ChIP and nuclear run-on assays are described in detail in the Methods.

Full Methods and any associated references are available in the online version of the paper at www.nature.com/nature.

Received 4 December 2009; accepted 16 April 2010.
Published online 13 June 2010.

1. Matzke, M. A. & Birchler, J. A. RNAi-mediated pathways in the nucleus. *Nature Rev. Genet.* **6,** 24–35 (2005).
2. Moazed, D. Small RNAs in transcriptional gene silencing and genome defence. *Nature* **457,** 413–420 (2009).
3. Guang, S. *et al.* An Argonaute transports siRNAs from the cytoplasm to the nucleus. *Science* **321,** 537–541 (2008).
4. Montgomery, M. K., Xu, S. & Fire, A. RNA as a target of double-stranded RNA-mediated genetic interference in *Caenorhabditis elegans*. *Proc. Natl Acad. Sci. USA* **95,** 15502–15507 (1998).
5. Clark, S. G., Lu, X. & Horvitz, H. R. The *Caenorhabditis elegans* locus *lin-15*, a negative regulator of a tyrosine kinase signaling pathway, encodes two different proteins. *Genetics* **137,** 987–997 (1994).
6. Huang, L. S., Tzou, P. & Sternberg, P. W. The *lin-15* locus encodes two negative regulators of *Caenorhabditis elegans* vulval development. *Mol. Biol. Cell* **5,** 395–411 (1994).
7. Tatusov, R. L. *et al.* The COG database: an updated version includes eukaryotes. *BMC Bioinformatics* **4,** 41–55 (2003).
8. Djupedal, I. *et al.* RNA Pol II subunit Rpb7 promotes centromeric transcription and RNAi-directed chromatin silencing. *Genes Dev.* **19,** 2301–2306 (2005).
9. Moore, M. J. & Proudfoot, N. J. Pre-mRNA processing reaches back to transcription and ahead to translation. *Cell* **136,** 688–700 (2009).
10. Rogalski, T. M., Golomb, M. & Riddle, D. L. Mutant *Caenorhabditis elegans* RNA polymerase II with a 20,000-fold reduced sensitivity to α-amanitin. *Genetics* **126,** 889–898 (1990).
11. Liu, J. *et al.* Argonaute2 is the catalytic engine of mammalian RNAi. *Science* **305,** 1437–1441 (2004).
12. Yigit, E. *et al.* Analysis of the *C. elegans* Argonaute family reveals that distinct Argonautes act sequentially during RNAi. *Cell* **127,** 747–757 (2006).
13. Duchaine, T. F. *et al.* Functional proteomics reveals the biochemical niche of *C. elegans* DCR-1 in multiple small-RNA-mediated pathways. *Cell* **124,** 343–354 (2006).
14. Lee, R. C., Hammell, C. M. & Ambros, V. Interacting endogenous and exogenous RNAi pathways in *Caenorhabditis elegans*. *RNA* **12,** 589–597 (2006).

Supplementary Information is linked to the online version of the paper at www.nature.com/nature.

Acknowledgements We thank P. Anderson, members of the Anderson laboratory, D. Wassarman and D. Brow for comments, and the *Caenorhabditis* Genetics Center for strains. This work was supported by grants from the Pew and Shaw scholars programmes, the National Institutes of Health and the American Heart Association.

Author Contributions S.G. performed genetic screening, generated constructs and contributed to Figs 1a, 2b, c, 3b, e, 4a and Supplementary Figs 2, 6, 7 and 9–12. A.F.B. mapped *nrde-2*, generated transgenic lines and contributed to Fig. 1c, d and Supplementary Figs 3 and 5. K.B.B. contributed to Fig. 1b and Supplementary Figs 3 and 8. N.B. contributed to Fig. 3a and Supplementary Fig. 8. D.M.P. contributed to Fig. 2a. S.K. wrote the paper and contributed to Figs 2d, 3c, d, 4b–d and Supplementary Figs 1, 2, 13 and 14.

Author Information Reprints and permissions information is available at www.nature.com/reprints. The authors declare no competing financial interests. Readers are welcome to comment on the online version of this article at www.nature.com/nature. Correspondence and requests for materials should be addressed to S.K. (sgkennedy@wisc.edu).

METHODS

Strains. The following strains were used for this work: (YY151) *eri-1(mg366); nrde-2(gg091)*, (YY158) *nrde-3(gg066)*, (YY174) *ggIS1*[*nrde-3p::3xflag::gfp::nrde-3*], (YY178) *eri-1(mg366); ggIS1*, (YY186) *nrde-2(gg091)*, (YY197) *nrde-2(gg091)*; *axIs36*[*pes-10::gfp*], (YY229) *nrde-2(gg091); ggIS1*, (YY258) *nrde-2(gg091); nrde-3(gg066)*, (YY298) *nrde-3(gg066); ggIS24*[*nrde-3p::3xflag::gfp::nrde-3*nls*], (YY323) *eri-1(mg366); nrde-2(gg091); unc-119(ed3); ggIS28*[nrde-3p::3xflag::gfp::nrde-2], (YY346), *nrde-2(gg091); ggIS28*, (YY353) *nrde-2(gg091); ggIS1*; *ggIS36*[*nrde-3p::3xha::gfp::nrde-2*], (YY363) *nrde-3(gg066); nrde-2(gg091); ggIS28*, (GR1373) *eri-1(mg366)*, (WM27) *rde-1(ne219)*, (DR1099) *ama-1(m118m526)*, (MT309) *lin-15AB(n309)*, (JH103) *axIs36*.

RNAi. RNAi experiments were conducted as described previously[15]. Basically, dsRNA-expressing bacteria, including *lir-1*, *pos-1* and *unc-15*, were obtained from the Ahringer RNAi library[16] and were sequenced to verify their identities. The *lin-15b* RNAi clone was described previously[3]. The *lin-15b* dsRNA (clone 2, Supplementary Fig. 14) targeting nucleotides 5–524 of *lin-15b* was constructed by PCR amplification of genomic DNA with primers (5′-gctaAAGCTT atgcaaacgctaaaaa-3′ and 5′-gctaAAGCTTcgtcctcatctccaaca-3′), inserted into the HindIII site of L4440 plasmid (a gift from A. Fire), and transformed into HT115 *Escherichia coli*. The *unc-40* RNAi clone was constructed by PCR amplification of *unc-40* exons 5–7 from genomic DNA with primers (5′-ttt AAGCTTaacagcagtttggcttcacaacg-3′ and 5′-tttAAGCTTttcggctcaattacaaaatactcgc -3′), inserted into the HindIII site of L4440 plasmid. The *dpy-28* RNAi clone was constructed by PCR amplification of *dpy-28* exon 5 with primers (5′-tttAAGCTTcgaaacgtgcttcaactag-3′ and 5′-tttAAGCTTatgtccatgtcgattattatcc-3′), and inserted into the HindIII site of L4440 plasmid.

***lir-1* RNAi.** Both *lir-1* and *lin-26* are co-transcribed in an operon. Loss of function mutations in *lin-26*, but not *lir-1*, are lethal[17]. RNAi targeting *lir-1* is lethal, indicating that RNAi silences the nuclear-localized *lir-1/lin-26* polycistronic RNA[3,17]. *eri-1*(−) animals exhibit enhanced sensitivity to dsRNAs[18]. Therefore an *eri-1*(−) genetic background was used to facilitate phenotypic analysis in Fig. 1b. The *lir-1* RNAi elicits lethality in *eri-1*(+) animals that is less pronounced than in *eri-1*(−) animals (not shown). The lethality of *lir-1* RNAi in *eri-1*(+) animals is also NRDE-2/3-dependent (not shown).

RNA isolation. RNA was isolated by TRIzol extraction from whole animals or hypochlorite-isolated embryos, as indicated. RNA was pelleted by isopropanol precipitation, resuspended in 100 µl RNA IP buffer (20 mM Tris-HCl, pH 7.5, 200 mM NaCl, 2.5 mM $MgCl_2$, 0.5% NP-40 and 10% glycerol), and incubated with 2 µl Turbo DNase I (Ambion) at 37 °C for 20 min. RNA was re-purified by TRIzol followed by isopropanol precipitation, and resuspended in water and converted to cDNA for quantitative rtPCR analysis. Samples were normalized to *eft-3* pre-mRNA. *lin-15b* RNAi directed a significant, but less pronounced, NRDE-2-dependent silencing of *lin-15b* pre-mRNA in *eri-1*(+) animals than in *eri-1*(−) animals (not shown).

Construction of plasmids and transgenic strains. FLAG::GFP::NRDE-3 and FLAG::GFP::NRDE-3(*NLS) were described previously[3]. To make pNRDE-3p::3×FLAG::GFP::NRDE-2, the *nrde-2* coding region and predicted *nrde-2* 3′ UTR were amplified by PCR from genomic N2 DNA with primers (5′-tttggtaccATGTTTCGAGCGTATGG and 5′-tttggtaccCTGTGCACATACATTGC) and inserted into the pSG082 plasmid 3′ to *nrde-3p*::3×FLAG::GFP. To make 3×HA::GFP-tagged NRDE-2, a 3×HA::GFP coding region was PCR amplified from pPD95.79 (a gift from A. Fire) with primers (5′-tttgtcgacTACCCA TACGATGTTCCAGATTACGCTTACCCATACGATGTTCCAGATTACGCTTA CCCATACGATGTTCCAGATTACGCTATGAGTAAAGGAGAAGAACTTTTC and 5′-aaagtcgacTTTGTATAGTTCATCC), digested with SalI and inserted into the XhoI site of the pPD##MM051 plasmid. Then, the 2.2-kilobase *nrde-3* promoter region was inserted into the HindIII site. The *nrde-2* coding region with its 3′ UTR was inserted into KpnI site as described above, to make a pNRDE-3p::3×HA::GFP::NRDE-2 fusion gene.

Low-copy integrated transgenes were obtained by biolistic transformation[19]. Both HA- and FLAG-tagged transgenic lines rescued *nrde-2(gg091)* animals for *lir-1* RNAi-mediated lethality and *lin-15b* RNAi-mediated multi-vulva formation.

Images were collected on a Zeiss Imager D1 microscope. Pictures of seam cells were taken from L3 stage animals.

In situ hybridization was performed as described previously[3].

Isolation and detection of NRDE-associated pre-mRNAs. NRDE-3 and NRDE-2 co-precipitating pre-mRNAs were purified from embryos with anti-FLAG M2 antibody (Sigma, A2220) as described previously[3]. Transcripts associated with RNAP II were isolated with the monoclonal antibody 8WG16 (Covance) and quantified as described previously for NRDE-3 co-precipitating pre-mRNAs[3].

Co-immunoprecipitation of NRDE-2 and NRDE-3. Hypochlorite-isolated embryos were sonicated in lysis buffer (20 mM Tris-HCl, pH 7.5, 200 mM NaCl, 2.5 mM $MgCl_2$, 0.5% NP-40 and 10% glycerol, with proteinase inhibitor tablet (Roche)). FLAG::GFP::NRDE-3 was immunoprecipitated with α-FLAG M2 antibody (Sigma, A2220) and eluted with FLAG peptide (final concentration 0.25 mg ml^{-1}). NRDE-2 was detected by western blotting with an affinity purified NRDE-2 antibody (WI329) generated in rabbits using the peptide KVVEADERRKNYKEI (Covance).

cDNA preparation. RNAs were converted to cDNA by the iScript cDNA Synthesis Kit (Bio-Rad, 170-8890) following the vendor's protocol.

ChIP. Hypochlorite-isolated embryos were cross-linked in 2% formaldehyde/M9 for 30 min at room temperature. Fixation was stopped by adding glycine to 0.125 M and incubating for 5 min. Embryos were washed twice in M9 and once in FA buffer (50 mM Tris/HCl pH 7.5, 1 mM EDTA, 1% Triton X-100, 0.1% sodium deoxycholate, 150 mM NaCl) and frozen on dry ice for 15 min. Embryos were resuspended in 1 ml FA buffer with proteinase inhibitor tablet (Roche), and sonicated 11 times for 10 s each by Branson Digital Sonifier at 10% output. Between each sonication, samples were put on dry ice/ethanol for 5 s, and then on ice. Lysates were centrifuged for 10 min at 4 °C. Supernatant was transferred to a new tube and pre-cleared with salmon-sperm-DNA-coated protein-A agarose beads (Upstate). Pre-cleared lysates were incubated with 4 µl anti-RNA polymerase II antibody, clone 8WG16 (Covance) or anti-trimethylated histone 3 lysine 9 (Upstate 07-523) for 2 h. BSA and salmon-sperm-DNA pre-treated protein-A agarose beads were added. Beads were pelleted and washed twice in FA buffer, twice in FA-500 buffer (50 mM Tris/HCl pH 7.5, 1 mM EDTA, 1% Triton X-100, 0.1% sodium deoxycholate, 500 mM NaCl), once in LiCl wash buffer (0.25 M LiCl, 1% NP-40, 1% sodium deoxycholate, 1 mM EDTA, 10 mM Tris-HCl, pH 8.0) and three times in TE buffer. Chromatin was eluted with two treatments of elution buffer (1% SDS, 0.1 M $NaHCO_3$) for 15 min each at room temperature. Eluants were combined, 30 µl 5 M NaCl was added and cross-links were reversed by heating at 65 °C for 4 h. DNAs were further purified using the QIAquick PCR Purification Kit (Qiagen) and analysed by quantitative rtPCR. ChIP data were normalized to co-immunoprecipitated *eft-3* promoter DNA.

Nuclear run-on assay. The nuclear run-on protocol is modified from ref. 20. Embryos were harvested by hypochlorite treatment and treated with 100 µl 2 U ml^{-1} chitinase (Sigma) at room temperature for 20 min. Embryos were rinsed once in M9 buffer and resuspended in 50 mM Tris-HCl, pH 7.5, 5 mM $MgCl_2$, 0.5% NP-40 and 10% glycerol. Embryos were dounced on ice with six strokes of pestle B, centrifuged at 4,000*g* and washed four times with 1 ml cold douncing buffer. Microscopic analysis indicated that these samples contained intact nuclei, cellular debris and some intact cells. These crude nuclei preps were resuspended in 100 µl nuclear run-on buffer (50 mM Tris-HCl, pH 7.5, 5 mM $MgCl_2$, 150 mM KCl, 0.1% sarkosyl and 10 mM DTT), 1 µl each of 10 mM ATP, GTP, CTP, 1 µl 10 mM BrUTP (Invitrogen) and 1 µl RNaseOUT (Invitrogen) with or without α-amanitin (Sigma, 5 µg ml^{-1}). Reaction mixtures were pre-incubated on ice for 3 min, then at 28 °C for 5 min. Run-on reactions were stopped by addition of 500 µl TRIzol (Invitrogen).

RNAs were isolated by TRIzol purification followed by isopropanol precipitation, resuspended in 100 µl RNA immunoprecipitation buffer (20 mM Tris-HCl, pH 7.5, 200 mM NaCl, 2.5 mM $MgCl_2$, 0.5% NP-40 and 10% glycerol), and incubated with 2 µl Turbo DNase I (Ambion) at 37 °C for 20 min. RNA was purified again by TRIzol followed by isopropanol precipitation, and resuspended in 500 µl RNA immunoprecipitation buffer. RNA was incubated with 2 µl anti-BrdU antibody (Invitrogen, A21300) in the presence of 2 µl RNaseOUT at 4 °C for 2 h, immunoprecipitated with 10 µl protein-G agarose beads (Santa Cruz), which was pre-coated with yeast transfer RNA, and washed five times with RNA immunoprecipitation buffer. Precipitated RNA was isolated by TRIzol extraction followed by isopropanol precipitation. RNA was converted to cDNA and quantified by rtPCR. Samples were normalized to *eft-3* transcription levels.

Quantitative rtPCR. Quantitative rtPCR primer sequences are available upon request.

15. Timmons, L., Court, D. L. & Fire, A. Ingestion of bacterially expressed dsRNAs can produce specific and potent genetic interference in *Caenorhabditis elegans*. *Gene* **263**, 103–112 (2001).
16. Kamath, R. S. *et al.* Systematic functional analysis of the *Caenorhabditis elegans* genome using RNAi. *Nature* **421**, 231–237 (2003).
17. Bosher, J. M., Dufourcq, P., Sookhareea, S. & Labouesse, M. RNA interference can target pre-mRNA: consequences for gene expression in a *Caenorhabditis elegans* operon. *Genetics* **153**, 1245–1256 (1999).
18. Kennedy, S., Wang, D. & Ruvkun, G. A conserved siRNA-degrading RNase negatively regulates RNA interference in *C. elegans*. *Nature* **427**, 645–649 (2004).
19. Berezikov, E., Bargmann, C. I. & Plasterk, R. H. Homologous gene targeting in *Caenorhabditis elegans* by biolistic transformation. *Nucleic Acids Res.* **32**, e40 (2004).
20. Core, L. J., Waterfall, J. J. & Lis, J. T. Nascent RNA sequencing reveals widespread pausing and divergent initiation at human promoters. *Science* **322**, 1845–1848 (2008).